

Supporting Information for:

**Anchoring a Molecular Iron Catalyst to Solar-Responsive WO₃
Improves the Rate and Selectivity of Photoelectrochemical Water
Oxidation**

*Benjamin M. Klepser and Bart M. Bartlett**

Department of Chemistry, University of Michigan, 930 North University Ann Arbor, MI United States

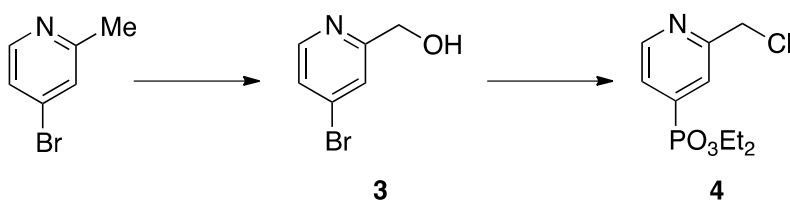
<i>Index</i>	<i>Page</i>
Experimental Section	S2
Figure S1. Solution electrochemistry of catalysts 1 and 2	S5
Figure S2. UV-Vis and Raman spectra of WO ₃ , 1 , and 1 -WO ₃	S6
Figure S3. Cyclic voltammetry of WO ₃ , 1 , and 1 -WO ₃	S6
Figure S4. Low temperature EPR of 1 after electrolysis	S7
Figure S5. Bulk Electrolysis to determine coverage of 1 on WO ₃	S8
Figure S6. Dark LSVs of 1 -WO ₃ and WO ₃ and CV of 1 -FTO	S8
Figure S7. Control LSVs of WO ₃ soaked only in acetonitrile, in FeCl ₂ , or tebppmcn	S9
Figure S8. SEM thickness of optimized WO ₃	S9
Figure S9. LSVs with thinner WO ₃	S10
Figure S10. LSVs varying pH on 1 -WO ₃	S11
Figure S11. Two Additional O ₂ evolution runs	S12
Figure S12. Faradaic efficiency of 1 -WO ₃ for 12 hours	S12
Figure S13. Faradaic efficiency of tebppmcn-WO ₃	S13
Figure S14. Fe 2p XPS of 1 -WO ₃ electrodes	S13
Figure S15. Faradaic efficiency of a single 1 -WO ₃ electrode subsequent runs	S14
Figure S16. Faradaic efficiency of a WO ₃ with 1 in solution	S14
Figure S17. ESI+ mass spectrometry of 1 -WO ₃ electrolyte after electrolysis	S15
Figure S18. CV of the concentrated electrolyte solution after photoelectrolysis.	S15
Figure S19. SEM of 1 -WO ₃ electrode before and after electrolysis	S16
Table S1. Faradaic efficiencies of O ₂ experiments for WO ₃ and 1 -WO ₃	S16

Experimental Section

General Methods

All reactions were carried out under a nitrogen atmosphere unless otherwise noted. THF, CH₃CN, and CH₂Cl₂ were dried prior to use according to common practices. All other materials were obtained from commercial sources, and used as purchased. Column chromatography was performed using standard 200 mesh silica gel. Elemental analyses were performed by Atlantic Microlab, Inc. for C, H, N, and Cl determinations. ¹HNMR and ¹³CNMR spectra were recorded in CDCl₃ or CD₃CN using a Varian MR400 at 400 MHz. Electrospray ionization mass spectra were collected on a Micromass LCT TOF MS through a Waters 1525 GC. UV/Visible/NIR spectroscopy was performed on an Agilent CaryWin 5000.

Synthesis



Preparation of **3**¹:

4-bromo-2-methylpyridine (4.30 g, 25.0 mmol) in 100 mL CHCl₃ was stirred with 70 wt% *m*-CPBA (8.01 g, 32.5 mmol) open to air for 2 hours. The reaction was quenched with 15 mL saturated NaHCO₃, and the resulting layers were separated. The aqueous layer was extracted with 30 mL CH₂Cl₂ (2×). The combined organic layers were washed with 30 mL of 2 M HCl, dried with Na₂SO₄, filtered, and concentrated.

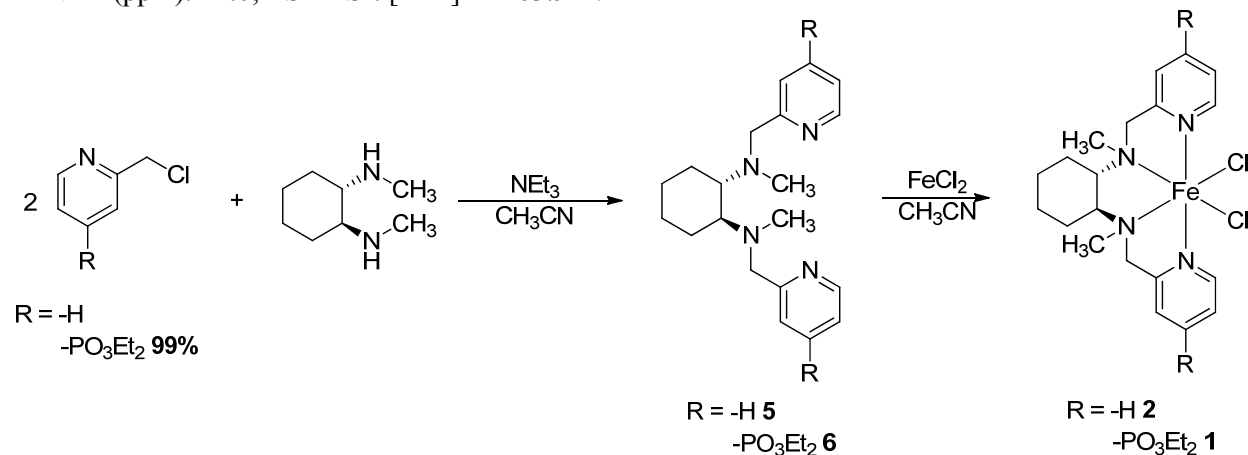
The resulting yellow oil was dissolved in 50 mL acetic anhydride and heated to 90 °C under air overnight. The dark solution was concentrated by vacuum distillation, and the residue was cooled to room temperature and dissolved in 30 mL methanol. The resulting solution was cooled to 0 °C. KOH (2.8 g, 50.0 mmol) was added to the chilled solution, and upon complete addition the ice bath was removed. The solution was warmed to room temperature and stirred for 3 hours. The reaction was concentrated under reduced pressure. The dark residue was taken up into 50 mL ethyl acetate and washed with saturated NaHCO₃. The aqueous layer was extracted with additional ethyl acetate (2× 50 mL) and the combined organic layers were dried with Na₂SO₄, filtered, and concentrated. The crude product was purified on silica with 50% ethyl acetate/hexanes. The desired alcohol **3** (2.04 g) was isolated in 43% yield over three steps. ¹HNMR(CDCl₃, ppm): 8.32 (d, 1H), 7.49 (s, 1H), 7.345 (d, 1H), 4.71 (s, 2H), 4.13 (broad, 1H); ¹³CNMR(ppm): 161.13, 149.17, 133.79, 125.78, 124.11, 63.91; ESI-MS⁺: [**3**+H]⁺ = 187.2 m/z

Preparation of **4**^{1,2}:

Palladium acetate (8.5 mg, 0.038 mmol), dppf (42.0 mg, 0.076 mmol), and KOAc (16 mg, 0.17 mmol) were dissolved in 5 mL THF. Triethylamine (0.27 mL, 1.9 mmol) was added to the reaction and the solution was heated to 70 °C under N₂ for 15 minutes. To the hot reaction, diethyl phosphite (0.16 mL, 1.27 mmol) and 4-bromo-2-(hydroxymethyl)pyridine (250 mg, 1.33 mmol) were added and the reaction was refluxed overnight. The reaction was cooled to room temperature and the reaction was concentrated under reduced pressure.

The crude residue was then taken into 5 mL of CH₂Cl₂ and cooled to 0 °C. Thionyl chloride (0.27 mL, 3.70 mmol) in 3 mL CH₂Cl₂ was added dropwise over 5 minutes. The resulting suspension was warmed to room temperature and stirred for 4 hours in air. The reaction was concentrated, and the brown residue was taken into 25 mL CH₂Cl₂ and washed with 25 mL saturated NaHCO₃. The resulting aqueous layer was extracted with CH₂Cl₂ (2× 25 mL) and the combined organic layers were washed with brine. Finally,

the organic layer was dried with Na₂SO₄, filtered, and concentrated under reduced pressure. This yielded the desired product **4** (239 mg) as a brown residue that was sufficiently pure by NMR in 72% yield over two steps. ¹HNMR(CDCl₃, ppm): 8.68 (t, 1H), 7.80 (d 1H), 7.57 (dd, 1H), 4.68 (s, 2H), 4.13 (m, 4H), 1.31 (t, 6H); ¹³CNMR(ppm): 157.10, 149.69, 139.81, 124.535, 124.34, 62.835, 46.20, 16.30; ³¹PNMR(ppm): 14.0; ESI-MS⁺: [4+H]⁺ = 263.9 m/z



General Preparation of **5** or **6**:

5: “bpmcn” R = H ¹HNMR(CDCl₃, ppm): 8.46 (dd, 2H), 7.545 (m, 4H), 7.08 (q, 2H), 3.83 (q, 4H), 2.635 (d, 2H), 2.27 (s, 6H), 1.955 (d, 2H), 1.735 (d, 2H), 1.28 (d, 2H), 1.13, (d, 2H); ¹³CNMR(ppm): 161.44, 148.57, 136.17, 122.77, 121.48, 64.56, 60.46, 36.62, 25.84; ESI-MS⁺: [6+H]⁺ = 323.8 m/z

6: “tebppmcn” R = PO₃Et₂

The racemic cyclohexane diamine (54 mg, 0.38 mmol) was dissolved in 5 mL of acetonitrile. Triethylamine (0.16 mL, 1.13 mmol) and **4** (199 mg, 0.76 mmol) were added to the stirring solution. The reaction was heated to 100 °C and attached with a long reflux condensor. After heating the reaction overnight, it was cooled to room temperature and concentrated under reduced pressure. The residue was dissolved in 10 mL CH₂Cl₂ and washed with 10 mL saturated NaHCO₃. The aqueous layer was extracted an additional 2 times with CH₂Cl₂. The combined organic layers were dried with Na₂SO₄, filtered, and concentrated. The crude product was purified on silica with 86% ethyl acetate, 10% methanol, and 4% conc. NH₄OH (R_f ~0.5). Fractions collected from the column were dried with Na₂SO₄, filtered, and concentrated under reduced pressure. This yielded an orange oil (173 mg, 58%). ¹HNMR(CDCl₃, ppm): 8.58 (t, 2H), 7.875 (d, 2H), 7.455 (q, 2H), 4.09 (m, 8H), 3.91 (s, 4H), 2.575 (d, 2H), 2.28 (s, 6H), 1.875 (d, 2H), 1.68 (d, 2H), 1.25 (m, 14H), 1.07 (t, 2H); ¹³CNMR(ppm): 148.98, 138.52, 136.69, 124.41, 123.22, 63.95, 62.63, 60.86, 36.78, 26.93, 25.64, 16.27; ³¹PNMR 15.26; ESI-MS⁺: [5+H]⁺ = 597.0 m/z⁺

General Preparation of **1** or **2**³:

1.0 eq. of ligand was added to 5 mL acetonitrile under N₂. To the stirring solution, 1.0 eq. of anhydrous FeCl₂ was added, and the reaction immediately turned from orange to purple (**1**) or yellow (**2**). The reaction was stirred overnight and concentrated under reduced pressure. If a precipitate was present, the solid was isolated as the pure product (**2**) and rinsed with diethyl ether. If no precipitate formed, the solution was concentrated and dried in a vacuum oven, yielding the pure complex. X-ray quality crystals were obtained by slow diffusion of ether into a concentrated solution of the complex in CH₃CN.

1: ¹HNMR(CD₃CN, ppm): 108.3, 62.07, 51.92, 51.39, 14.90, 8.0, 3.94, 2.01, 1.43, 0.16, -2.18, -2.85, -11.73; ESI-MS⁺: [Fe(tebppmcn)Cl(CH₃CN)]⁺ = 721.4 m/z⁺; [Fe(tebppmcn)(Cl)_{1.7}(HO)_{0.3}•0.7H₂O] EA: (theory) C 46.12, H 6.59, N 7.68, Cl 8.10; (found) C 45.27, H 6.47, N 7.67, Cl 8.06

2: ¹HNMR(CD₃CN, ppm): 109.48, 63.25, 54.58, 51.27, 20.43, 15.46, 3.17, 2.49, 1.98, 0.10, -19.03; ESI-MS⁺: [Fe(bpmcn)Cl(CH₃CN)]⁺ = 423.4 m/z⁺, [Fe(bpmcn)Cl₂•0.5H₂O] EA: (theory) C 52.20, H 6.35, N 12.17, Cl 15.41; (found) C 52.10, H 6.29, N 12.21, Cl 15.13

WO₃ was prepared by a previously reported method.⁴

Modification of WO₃ with **1**:

WO₃ electrodes were heated to 80 °C in a 500 μM **1**/acetonitrile solution and sealed in a vial. The anodes were soaked for 8 hours in the dark and then rinsed with excess acetonitrile and dried with N₂. This procedure resulted in a light yellow tint to the modified electrodes.

Electrochemistry

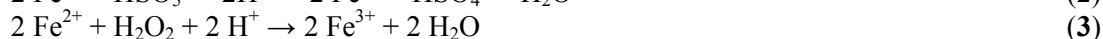
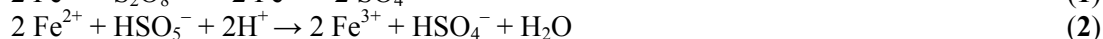
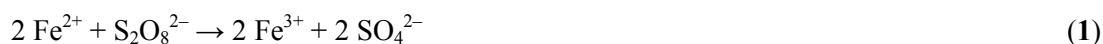
All electrochemistry was performed on either a CH Instruments CHI-600 or CHI-1000 potentiostat. All potentials are referenced to SCE (saturated calomel electrode) with saturated KCl electrolyte reference electrode (RE), and Pt was used as the counter electrode (CE) in all experiments. Non-aqueous solvents were dried prior to use and TBAPF₆ was recrystallized from EtOH prior to use. Glassy carbon (GC) was used as the working electrode (WE) for solution-based electrochemistry. Aqueous solutions were prepared using 18.2 Ω Milli-pore H₂O and concentrated sulfuric acid, and then pH adjusted with 7 M NaOH to obtain the desired concentration and pH. The aqueous solutions were also purged with N₂ prior to use, but were not sealed under N₂. All photoelectrochemical measurements were carried out in custom-built cells with quartz viewing windows. All illumination was carried out using a Newport Oriel 150 W Xe lamp fitted with an AM1.5G filter from Newport whose power was adjusted to 100 mW/cm².

Faradaic Efficiency: Oxygen Detection

Oxygen was quantified using a FOSSPOR fluorescence probe using two-point calibration at 20.90% and 0.00% O₂. O₂ evolution experiments were carried out in a custom-built two-sided cell with quartz windows, where the O₂ probe, working electrode, and reference electrode were on one side, with the temperature probe and the Pt auxiliary electrode on the other side. The solutions were purged with N₂ overnight, and then sealed under N₂ on a Schlenk line. The photoelectrode was illuminated at 100 mW/cm² filtered with AM 1.5G and the potential was held at 809 mV vs. SCE in pH 3 Na₂SO₄ (1.23 V vs. NHE). After collecting a stable 0% baseline for ~30 minutes, the photoanode was illuminated for ~3 hours. Following illumination, the O₂ was allowed to reach a stable O₂ level for ~30 minutes to allow for temperature fluctuations with the probe. Finally, the run was successful if the O₂ returned near 20.90% after re-exposing the O₂ probe to air. Faradaic efficiency was determined by dividing the measured moles of O₂ by the theoretical yield, determined by dividing the total charge passed during the experiment by 4F (4-electron oxidation, F = 96,485.34 C/mol e⁻).

Faradaic Efficiency: Non-oxygen Detection

Non-oxygen by-products from photoelectrolysis were measured by quantifying the amount of Fe²⁺ that was oxidized by the non-O₂ oxidants in solution (mainly S₂O₈²⁻, HSO₅⁻, and H₂O₂) according to the following reactions.



The amount of Fe^{3+} generated in the second reaction was quantified by addition of excess $\text{Na}(\text{SCN})$. The amount of Fe^{3+} generated was determined using Beer's law and 1 mol of Fe^{3+} was generated for every 1 mol of e^- not used to oxidize water completely, and thus the Faradaic efficiency of the cells for non- O_2 production was measured. To perform the reaction, 2.0 mL of 5 mM FeSO_4 in 100 mM pH 3 Na_2SO_4 and 1.0 mL of the test solution were mixed and equilibrated for 15 minutes to allow for the reaction to go to completion. NaSCN was added to the solutions (~ 40 mM) to generate the deep red $[\text{Fe}(\text{SCN})_6]^{3-}$ species, detectable by UV-Vis spectroscopy ($\epsilon = 172 \text{ M}^{-1} \text{ cm}^{-1}$ at $\lambda_{\text{max}} = 465 \text{ nm}$). The measurement was standardized using $\text{Ce}(\text{HSO}_4)_4$. If the reactions were not carried out in aerated solutions and during the time frame of the experiments then the detected concentrations of the non- O_2 oxidants was significantly diminished.

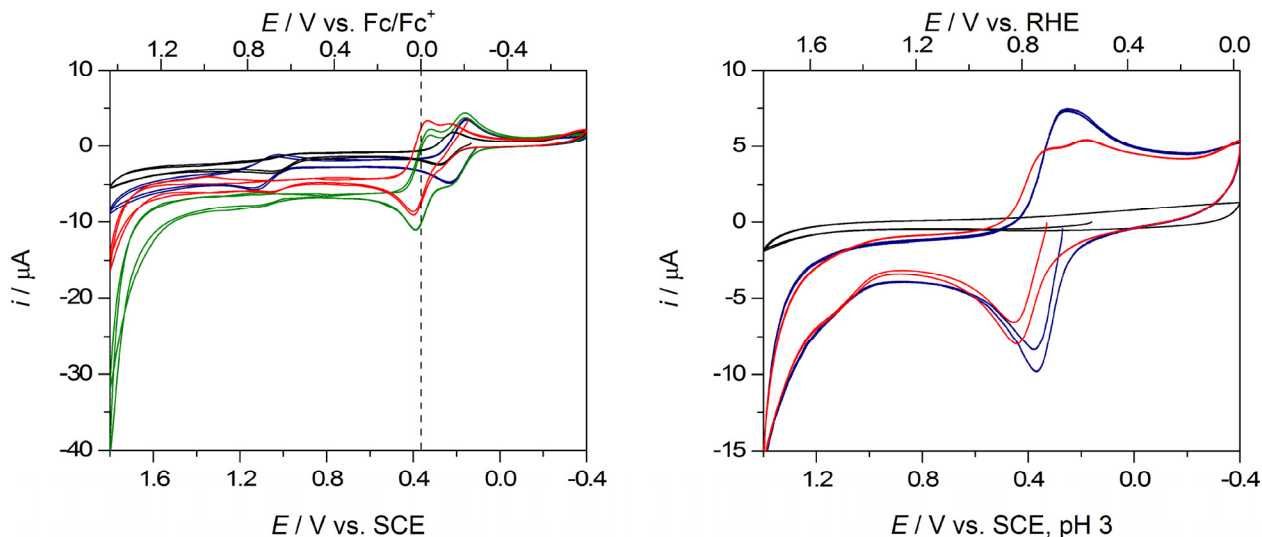


Figure S1. Left: Solution electrochemistry of 0.5 mM catalyst **1** (black) and **2** (blue) in 100 mM TBAPF_6 CH_3CN without Fc; 0.5 mM **1** (red) and **2** (green) with 0.5 mM Fc at 20 mV/s; Right: 1 mM **1** (red) or **2** (blue) in 100 mM Na_2SO_4 pH 3 (blank = black) at 50 mV/s using GC WE, SCE RE, Pt CE.

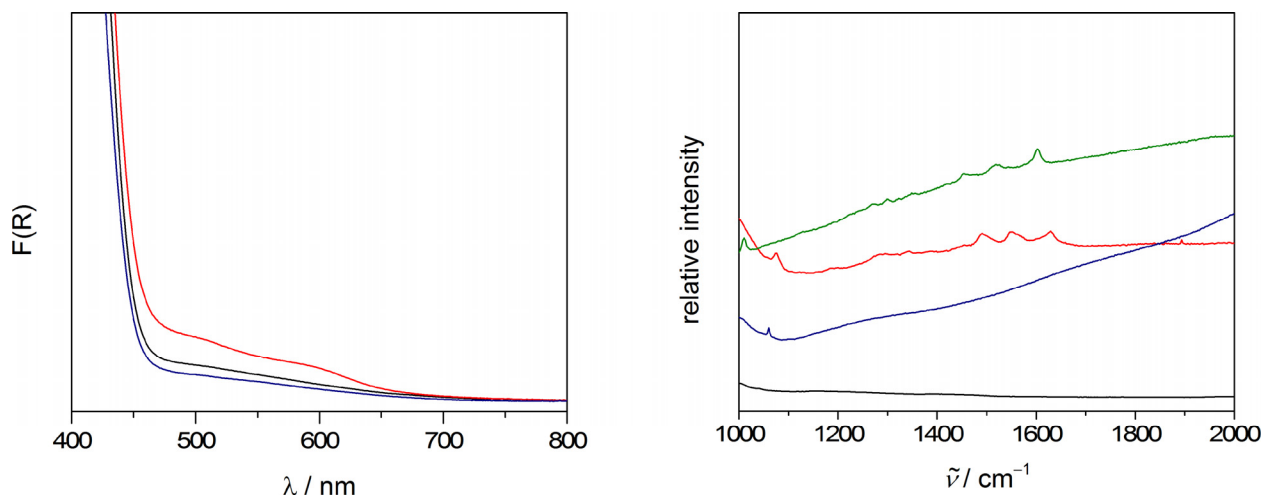


Figure S2. Left: Diffuse reflectance spectroscopy of WO₃ film (black), 1-WO₃ before electrolysis (red) and after electrolysis (blue); Right: Raman spectroscopy of WO₃ electrode (black), 1-WO₃ before electrolysis (red), 1-WO₃ after electrolysis (blue), and 1 powder (green).

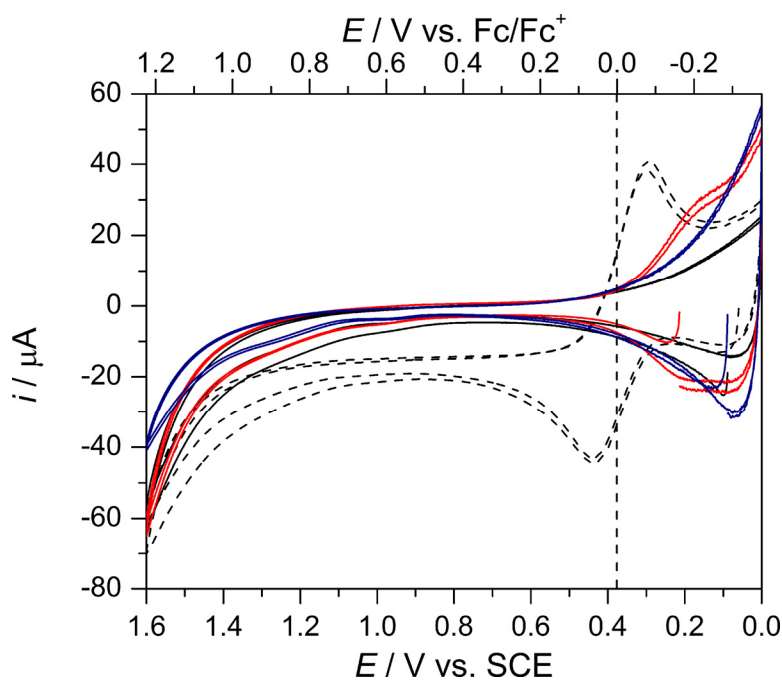


Figure S3. Cyclic voltammetry of bare WO₃ photoanode (black) with added Fc (dashed) and 1-WO₃ photoanode before LSVs (red) and after LSVs (blue) in 100 mM TBAPF₆ CH₃CN; CV's recorded at 20 mV/s with SCE RE and Pt CE in the dark.

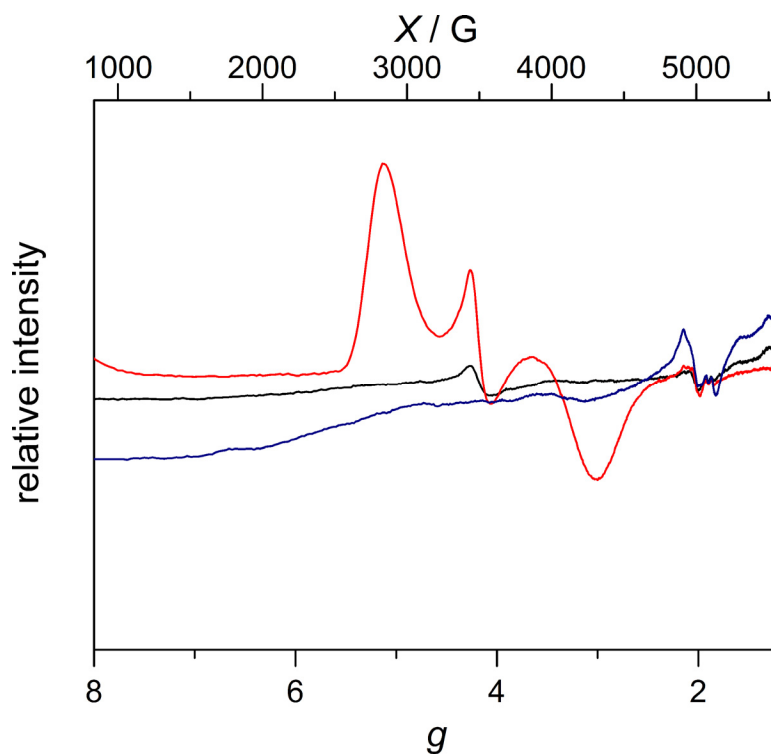


Figure S4. EPR at 4 K of 2.5 mM **1** in 100 mM TBAPF₆ CH₃CN at open circuit potential (black), after electrolysis at 0.6 V vs. SCE (red), and after electrolysis at 1.6 V vs. SCE (blue). Electrolysis was performed in a two compartment cell separated by a glass frit using a 1 cm² carbon felt electrode WE and SCE RE in one side with the 2.5 mM **1** solution and Pt mesh CE on the other side with blank electrolyte.

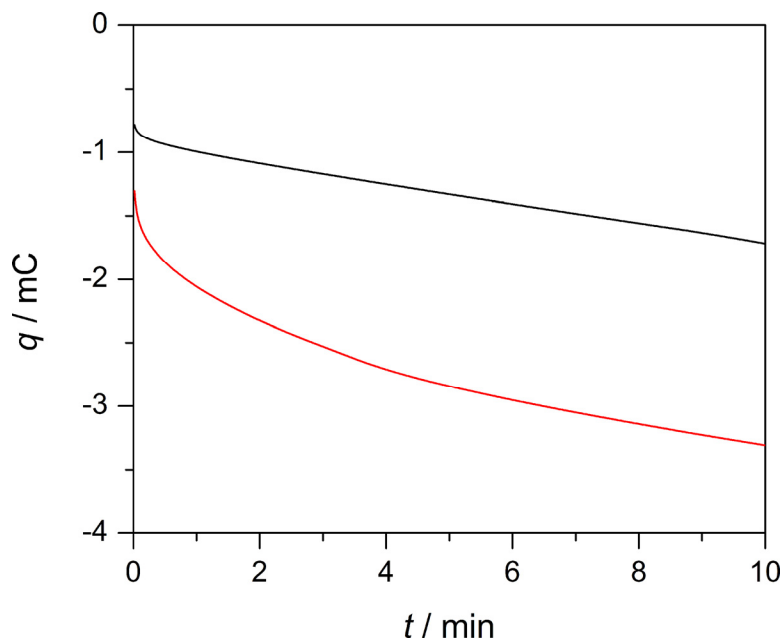


Figure S5. Bulk electrolysis (q vs. t) of bare WO_3 photoanode (black) and a typical **1**- WO_3 photoanode (red) before any other electrochemistry in 100 mM TBAPF_6 in CH_3CN ; potential held at 0.43 V vs. Fc^+/Fc^0 (0.8 V vs. SCE) with SCE RE and Pt CE in the dark. The coverage of **1** on this film was $15.65 \text{ nmol cm}^{-2}$ based on coulometry (i.e. after 5 minutes: $n = q/F = (0.00284 - 0.00133)/96,485 = 15.65 \times 10^{-9} \text{ moles e}^- \text{ passed} = 15.65 \times 10^{-9} \text{ moles Fe}^{2+} \text{ oxidized to Fe}^{3+}$)

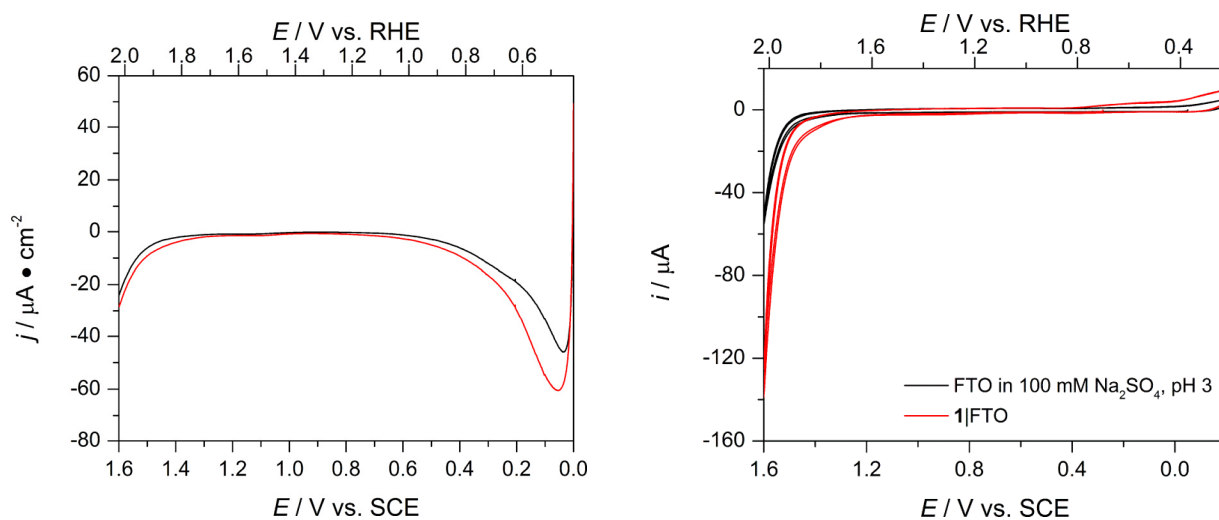


Figure S6. Left: Linear sweep voltammetry of bare WO_3 photoanode (black) and **1**- WO_3 photoanode (red) in 100 mM Na_2SO_4 pH 3; LSVs recorded at 20 mV/s with SCE RE and Pt CE in the dark. Right: CVs of **1**-FTO recorded under similar conditions.

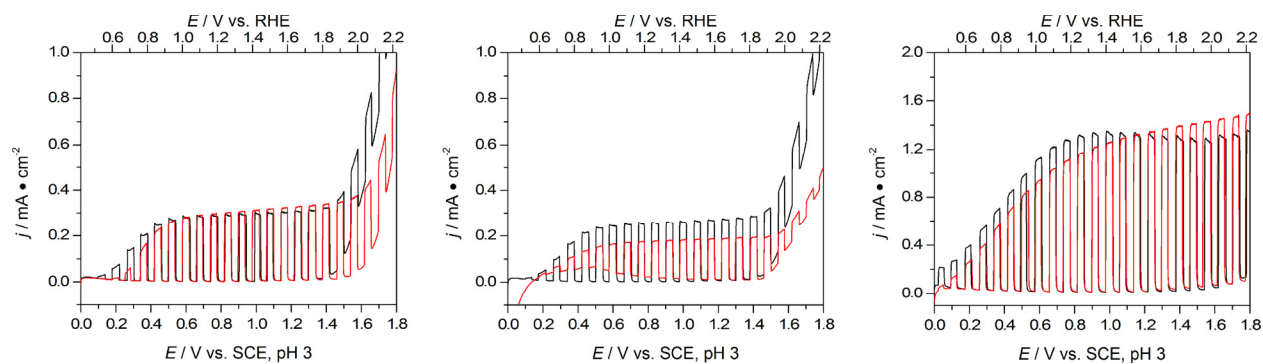


Figure S7. Left: Chopped-light LSV of a WO₃ film as prepared (black) and after soaking in CH₃CN (red); Middle: Chopped-light LSV of a WO₃ film as prepared (black) and after soaking with FeCl₂ (red); Right: Chopped-light LSV of a WO₃ film as prepared (black) and after soaking with tebppmcn (red) in pH 3 0.1 M Na₂SO₄, 100 mW cm⁻² AM 1.5G illumination, 20 mV/s, Pt CE, SCE RE.

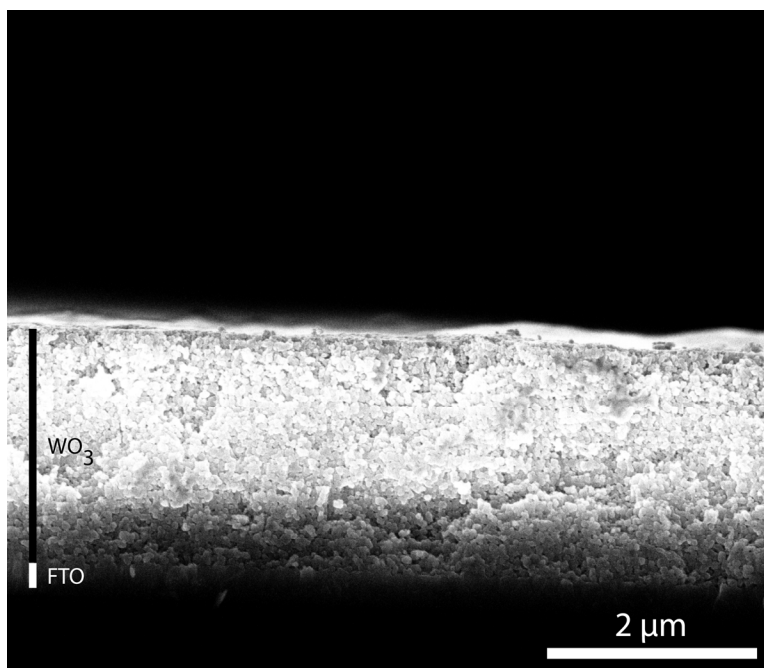


Figure S8. SEM of optimized WO₃ photoanodes with a thickness of ~1.8 μm whereas the thinner films were measured to be ~0.6 μm.

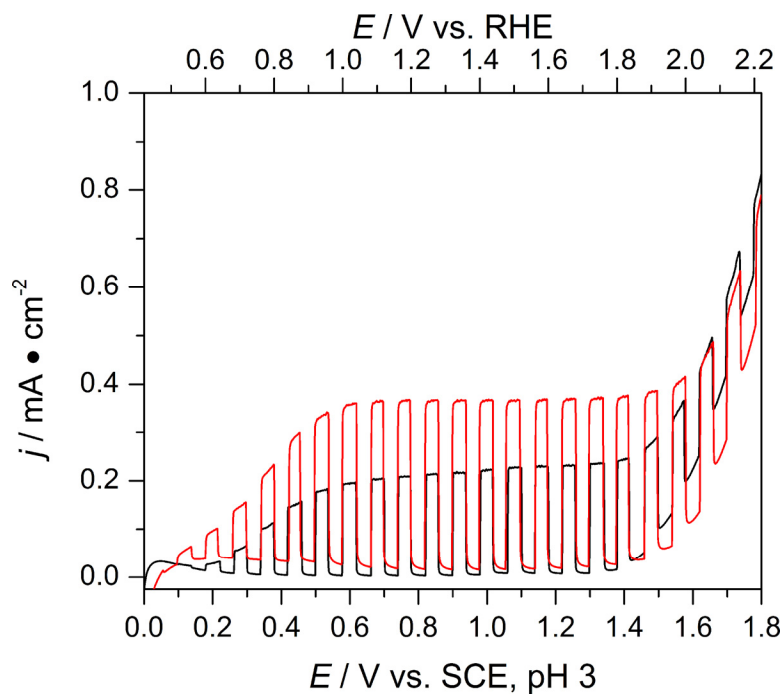


Figure S9. Chopped-light LSV of thinner photoanodes in 100 mM Na_2SO_4 at pH 3; SCE RE, Pt CE, 100 mW cm^{-2} , AM 1.5G with as prepared WO_3 (black) and $\mathbf{1}\text{-WO}_3$ (red).

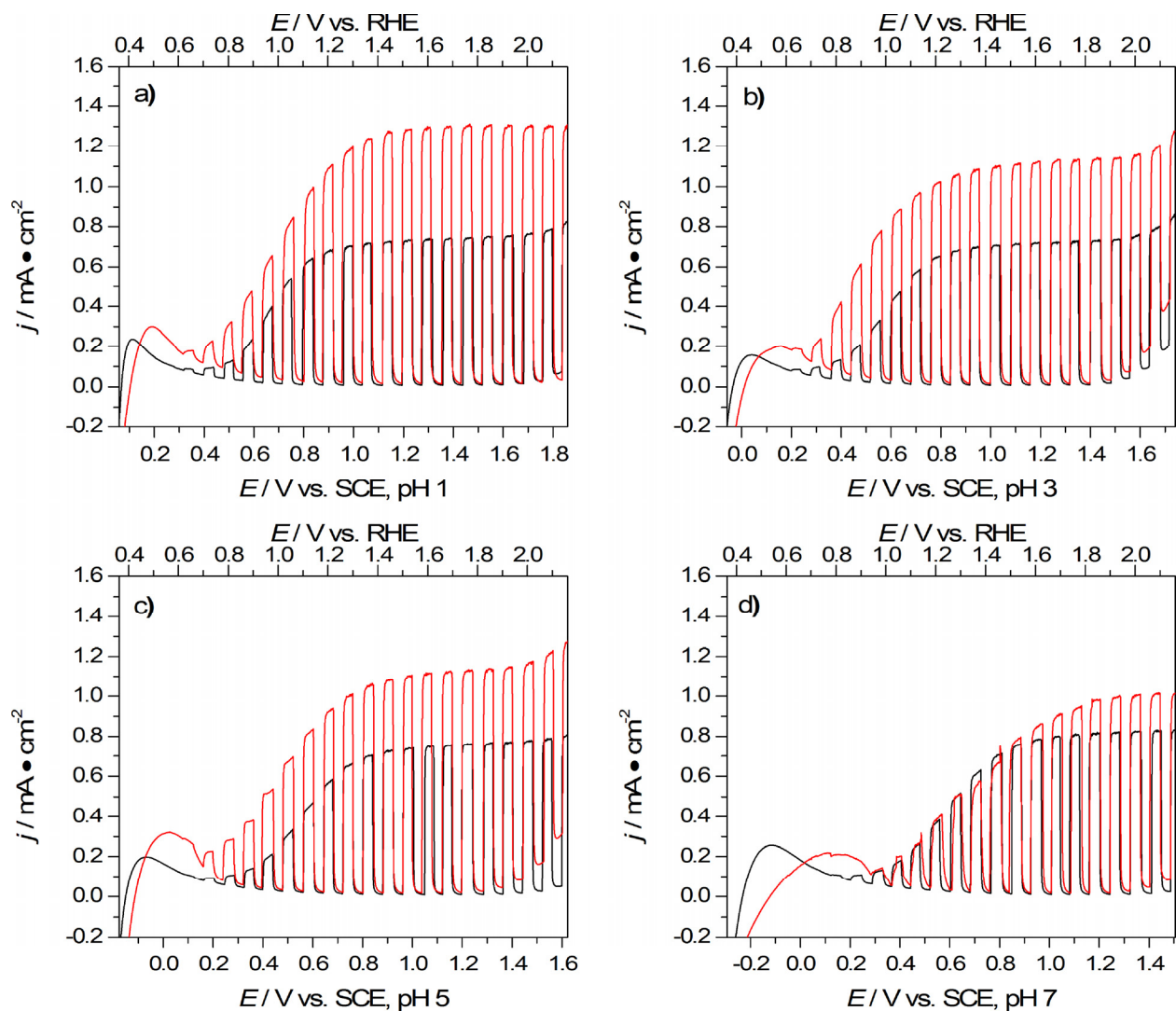


Figure S10. Chopped-light LSVs of photoanodes in 100 mM Na₂SO₄ at pH 1 (a), 3 (b), 5 (c), and 7 (d); SCE RE, Pt CE, 100 mW cm⁻², AM 1.5G with as prepared WO₃ (black) and 1-WO₃ (red).

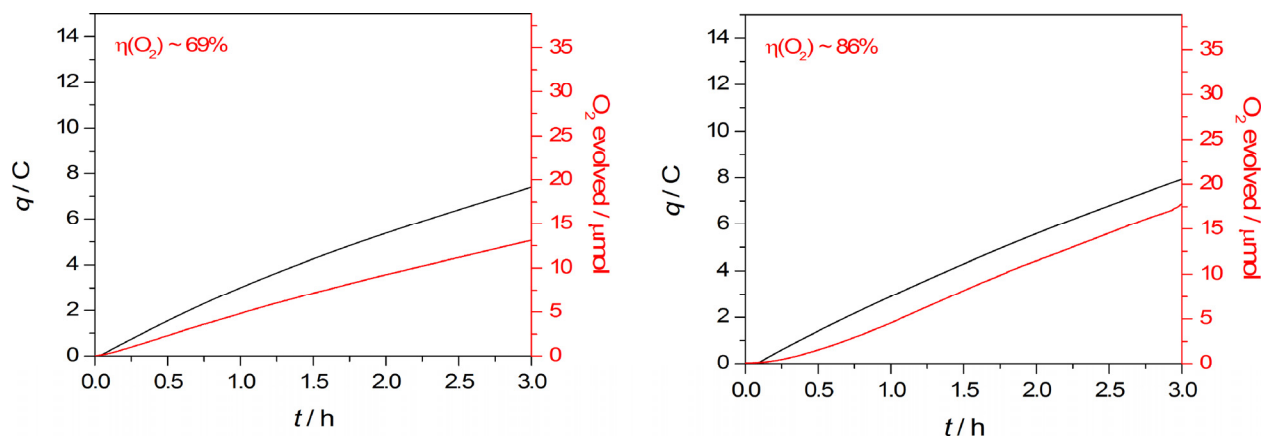


Figure S11. Additional Faradaic efficiency experiments of **1-WO₃** photoanodes in 100 mM Na₂SO₄ pH 3; potential held at 1.23 V vs. RHE, SCE RE, Pt CE with charge passed (black) and oxygen evolution (red).

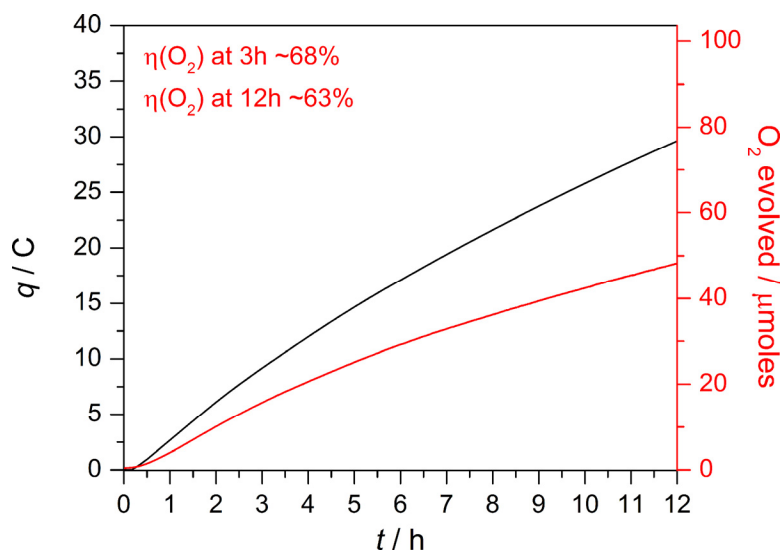


Figure S12. Faradaic efficiency of a **1-WO₃** photoanode in 100 mM Na₂SO₄ pH 3; potential held at 1.23 V vs. RHE, SCE RE, Pt CE for 12 hours with charge passed (black) and oxygen evolution (red).

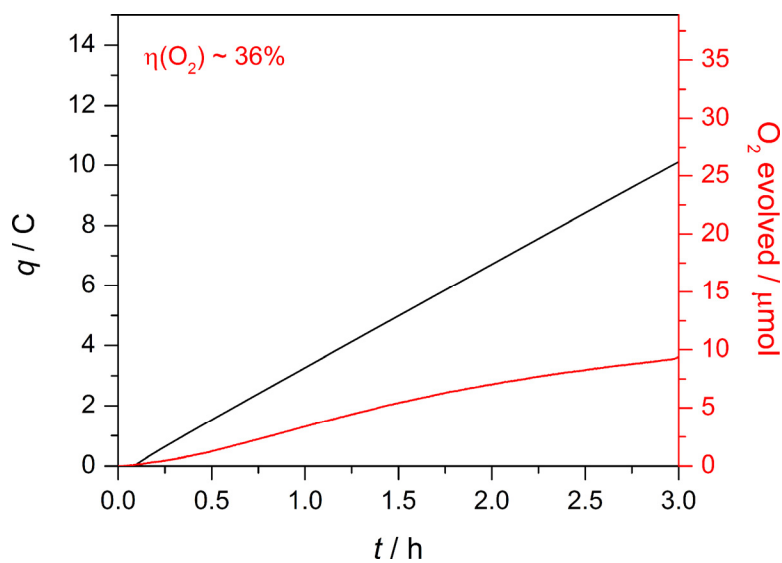


Figure S13. Faradaic efficiency of tebppmcn-WO₃ photoanode in 100 mM Na₂SO₄ pH 3; potential held at 1.23 V vs. RHE, SCE RE, Pt CE with charge passed (black) and oxygen evolution (red).

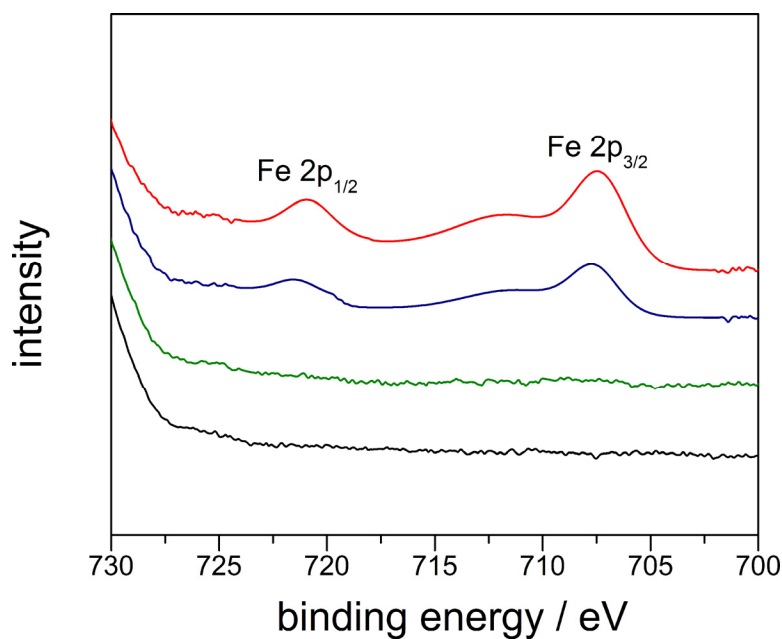


Figure S14. X-ray photoelectron spectrum of WO₃ photoanodes as prepared (black), freshly modified with **1** (red), after LSV of **1**-WO₃ in pH 3 Na₂SO₄ (blue), and after photoelectrolysis of **1**-WO₃ for 3 h (green).

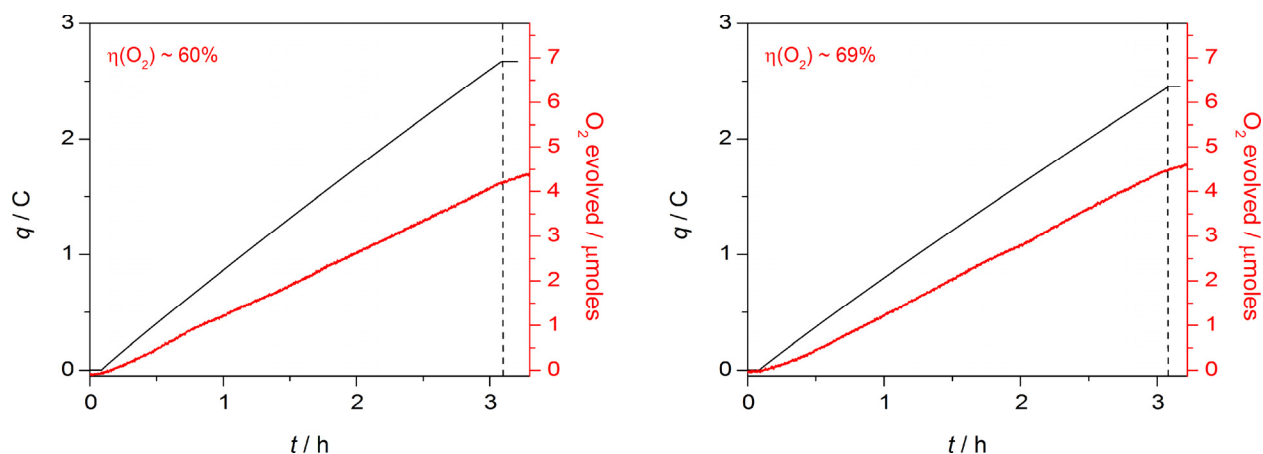


Figure S15. Left: First 3 h Faradaic efficiency experiment of a single **1**-WO₃ thinner photoanode in 100 mM Na₂SO₄ pH 3; Right: Second 3 h Faradaic efficiency experiment of a single **1**-WO₃ thinner photoanode in 100 mM Na₂SO₄ pH 3 when the potential was held at 1.23 V vs. RHE, SCE RE, Pt CE with charge passed (black) and oxygen evolution (red) the dashed line represents when the light is turned off in both plots.

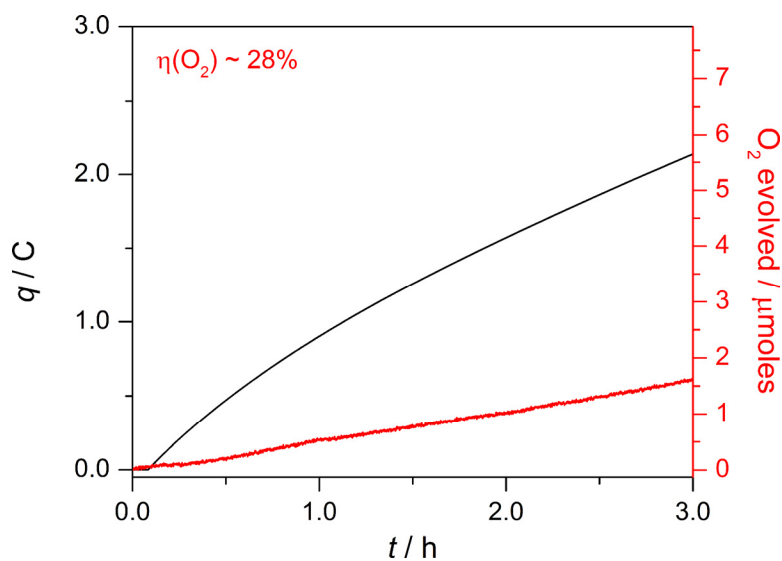


Figure S16. Faradaic efficiency of thinner WO₃ photoanode in 500 nM **1** and 100 mM Na₂SO₄ pH 3; potential held at 1.23 V vs. RHE, SCE RE, Pt CE with charge passed (black) and oxygen evolution (red).

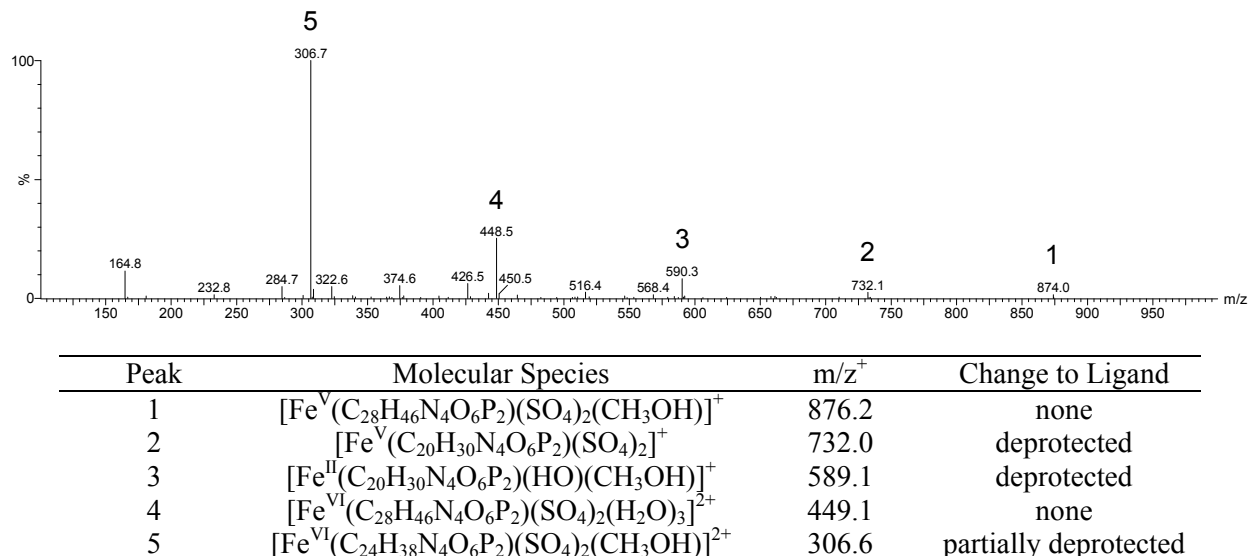


Figure S17. Positive electrospray ionization mass spectrometry of electrolyte after 3 hour photoelectrolysis with a 1-WO₃ photoanode in 100 mM Na₂SO₄ pH 3 at 1.23 V vs. RHE, SCE RE, Pt CE. Table includes major peak labels and the changes to the ligand. Minor peaks were also identified, but were not included for clarity.

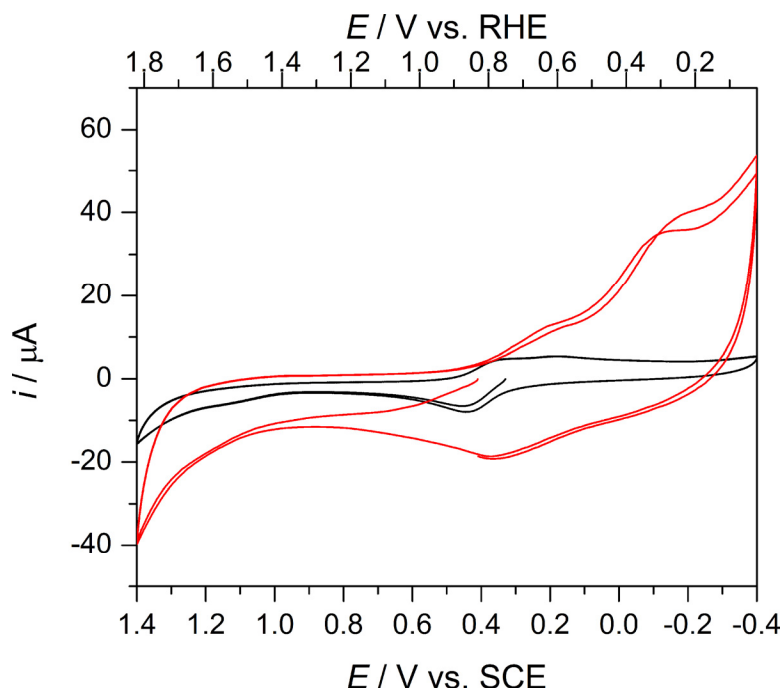


Figure S18. Cyclic voltammetry of 1 mM **1** in 100 mM Na₂SO₄ pH 3 (black) compared to a CV of a concentrated 100 mM Na₂SO₄ pH 3 solution containing **1** after a 3 hour photoelectrolysis with a 1-WO₃ photoanode (red) recorded with GC WE, SCE RE, and Pt CE at 50 mV/s.

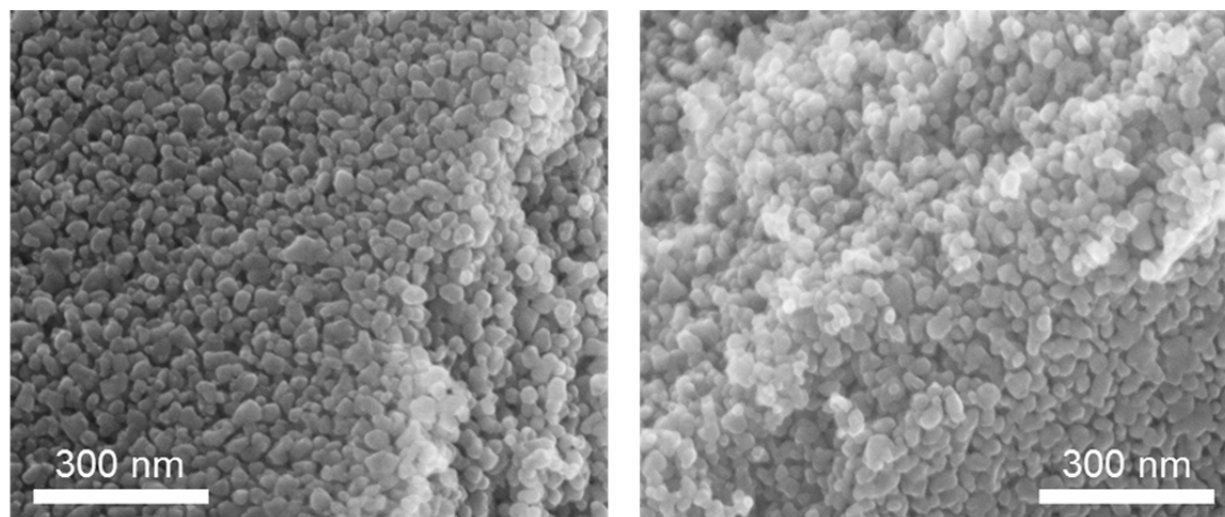


Figure S19. SEM of thinner **1**-WO₃ electrodes before (left) and after (right) 3 hour photoelectrolysis where the darker regions represent the plane or face of a larger aggregate on the electrode surface and the lighter regions are over the edge of the larger aggregates.

Table S1. Tabulated $\eta(\text{O}_2)$ % for different WO₃ and **1**-WO₃.

Entry	WO ₃	1 WO ₃	thinner WO ₃	thinner 1 WO ₃
1	53	83	45	62
2	64	86	30	57
3	52	69	38	63
4	—	—	20	64
mean	56	79	33	62
std. dev.	7	9	11	3

References

1. Deng, L.; Diao, J.; Chen, P.; Pujari, V.; Yao, Y. p Cheng, G.; Crick, D. C.; Prasad, B. V. V.; Song, Y. *J. Med. Chem.* **2011**, *54*, 4721-4734.
2. Kalek, M.; Jeowska, M.; Stawinski, J. *Adv. Synth. Catal.* **2009**, *351*, 3207-3216.
3. Costas, M.; Que, L. Jr. *Angew. Chem. Int. Ed.* **2002**, *41*, 2179-2181.
4. Santato, C.; Odziemkowski, M.; Ulmann, M.; Augustynski, J. *J. Am. Chem. Soc.* **2001**, *123*, 10639-10649.